COVER PAGE

Bibliographical reference

sonROAD18: Swiss Implementation of the CNOSSOS-EU Road Traffic Noise Emission Model, Kurt Heutschi, Barbara Locher and Michael Gerber, Acta Acustica **vol. 104** (Number 4), 2018, pp. 697-706

DOI

https://doi.org/10.3813/AAA.919209

Acta Acustica united with Acustica
Vol. 104 (2018) 697 – 706

DOI 10.3813/AAA.919209

sonROAD18: Swiss Implementation of the CNOSSOS-EU Road Traffic Noise Emission Model

Kurt Heutschi[1)], Barbara Locher[1)], Michael Gerber[2)]

[1)] Empa, Swiss Federal Laboratories for Materials Science and Technology, Laboratory for Acoustics/Noise Control, Ueberlandstrasse 129, 8600 Duebendorf, Switzerland. kurt.heutschi@empa.ch

[2)] Swiss Federal Office for the Environment, Bern, Switzerland

Summary

To account for recent developments in the fleet of road vehicles and to extend the allowable speed range, Switzerland has updated its road traffic noise emission model under the acronym *sonROAD18*. The model description is based on the formalism of CNOSSOS, however specified in third octave bands. In extension to the declaration of an average sound power radiated by a single vehicle, statistical indicators are provided as well to describe individual variations. Omnidirectional radiation characteristics is assumed in the horizontal plane whereby the emission is defined as equivalent sound power of a point source that induces a correct sound event level. In vertical direction, spectral corrections are applied to account for the reduced emission strength under large elevation angles. The accuracy of the model is specified for different scenarios with respect to the level of detail of available input parameters.

PACS no. 43.50.Lj

1. Introduction

The European initiative CNOSSOS [1] offers a framework for the emission and propagation calculation of the most important traffic noise sources: road, railway and air traffic. It aims at a harmonization of noise calculations in Europe and should replace national models when it comes to strategic noise mapping and the elaboration of action plans. It has evolved from the European research projects Harmonoise and Imagine [2]. In order to consider particular properties of the vehicle pool, a country-specific adaption of the model parameters is envisaged.

In Switzerland current road traffic noise models are StL-86+ [3] and sonRoad [4]. While StL-86+ is generally recommended, sonRoad is used in situations that are out of the scope of StL-86+, such as regimes with vehicle speeds below 50 km/h. Both calculation schemes will be replaced in near future by the emission model *sonROAD18* [5]. This update accounts for the recent changes in the vehicle fleet and will reduce prediction uncertainty. It will be coupled to an appropriate propagation model such as e.g. ISO 9613-2.

2. Model structure

sonROAD18 is based on the fundamental assumptions and empirical formulas of CNOSSOS.

Received 20 March 2018,
accepted 27 May 2018.

2.1. Fundamental Assumptions

Total noise emitted by a road vehicle splits up into propulsion and rolling noise. Both contributions are characterized by separate formulas that describe radiated power taking into account ground reflections in the vicinity of the source. For both sources a height of 0.05 m is assumed with the beneficial consequence that a vehicle can be described by one single point source.

2.2. Radiated sound power

2.2.1. Total sound power and variance of individual vehicles

The sound power level $L_W[c,i]$ of total radiated power of a vehicle of category c in the third octave band i is given as the energetic sum of the propulsion noise level $L_{W,P}$ and the rolling noise level $L_{W,R}$,

$$L_W[c,i] = 10\lg\left(10^{0.1L_{W,P[c,i]}} + 10^{0.1L_{W,R[c,i]}}\right) + \Delta L_{W,\theta}[c,i] + r[c]. \quad (1)$$

In extension to CNOSSOS, sonROAD18 considers in Equation (1) a vertical directivity $\Delta L_{W,\theta}[c,i]$ and with $r[c]$ a Gaussian distributed random number to statistically describe individual variation in emission strength. With $\sigma[c]$ as single vehicle standard deviation, $r[c]$ can be written as

$$r[c] = r_0[c] + n(\sigma[c]), \quad (2)$$

where $r_0[c] \approx -0.115\,(\sigma[c])^2$ is the difference between arithmetic and energetic mean value of a Gaussian level distribution. $n(\sigma[c])$ is a Gaussian distributed random number with mean = 0 and standard deviation = $\sigma[c]$.

It should be noted that the effect of individual vehicle speed variations is not included in $r[c]$ as this can be modeled by the speed dependent emission formula itself. For $r[c] = 0$ and for a given vehicle speed, $L_W[c]$ indicates the average sound power level of a vehicle in category c.

With knowledge of vehicle speed statistics and emission strength variation, distributions of noise level maxima can be predicted [6].

2.2.2. Propulsion noise

Sound power level of the propulsion noise contribution is described as

$$L_{W,P}[c,i] = A_P[c,i] + B_P[c,i]\frac{v - v_{\text{ref}}}{v_{\text{ref}}} + \Delta L_{W,P,\text{grad}}[c], \quad (3)$$

with vehicle speed v and $v_{\text{ref}} = 70\,\text{km/h}$ as a reference, $\Delta L_{W,P,\text{grad}}[c]$ is a correction for road gradients [1]. In contrast to CNOSSOS, sonROAD18 goes without an integral correction for accelerating driving conditions. If required, more sophisticated approaches [7],[8] or pass-by simulations with increased engine load are applied. This can be based on the assumption that an acceleration can be converted into an equivalent road gradient.

2.2.3. Rolling noise

Sound power level of the rolling noise contribution is described as

$$L_{W,R}[c,i] = A_R[c,i] + B_R[c,i]\,\text{lg}\left(\frac{v}{v_{\text{ref}}}\right) + \Delta L_{W,R,\text{road}}[i] + \Delta L_{W,R,\text{temp}}[c] + \Delta L_{W,R,\text{tyre}}[c,\text{pavement}], \quad (4)$$

with vehicle speed v and $v_{\text{ref}} = 70\,\text{km/h}$ as a reference. $\Delta L_{W,R,\text{road}}[i]$ represents the correction for the pavement. In sonROAD18 $\Delta L_{W,R,\text{road}}$ is considered a pavement property and as such defined independently of the vehicle category. $\Delta L_{W,R,\text{temp}}[c]$ describes the temperature dependency [1]. Deviating from CNOSSOS, a temperature of 10°C is assumed as a reference as this corresponds to the yearly average in Switzerland. $\Delta L_{W,R,\text{tyre}}[c,\text{pavement}]$ is a possible future correction to account for low noise tyres. The correction will depend on vehicle category and can only be put in connection with a specific pavement type.

3. Model parameter fitting

The adjustment of the model for the circumstances in Switzerland requires the determination of the vehicle category dependent spectra $A_P[c,i]$, $B_P[c,i]$, $A_R[c,i]$, $B_R[c,i]$ and the spectral pavement corrections $\Delta L_{W,R,\text{road}}[i]$.

Table I. Vehicle categories c according to the SWISS-10 classification scheme and equivalent CNOSSOS classes.

c	description	CNOSSOS
1	buses	3
2	motorcycles	4b
3	passenger cars	1
4	passenger cars w. trailer	1
5	delivery vans ≤ 3.5t	1
6	delivery vans ≤ 3.5t w. trailer	1
7	delivery vans ≤ 3.5t w. semitrailer	1
8	heavy goods vehicle HGV	3
9	HGV w. trailer	3
10	HGV articulated	3

3.1. Vehicle categories

Table I shows the vehicle categorization used in Switzerland [9] and the corresponding equivalent CNOSSOS classes. It should be noted that an allocation of SWISS10-cat8 (HGV) to CNOSSOS is not well-defined as lighter vehicles would rather correspond to CNOSSOS class 2 [10]. In situations where only limited information about the traffic flow is available, a SWISS10-converter can be used to break down total traffic volumes into different vehicle categories. In the future, the vehicle classification scheme will be extended to electric buses (1b), hybrid and electric passenger cars (3b, 3c) and to electric HGVs (11).

3.2. Evaluation of measurement data

The model parameters $A_P[c,i]$, $B_P[c,i]$, $A_R[c,i]$, $B_R[c,i]$ and $\Delta L_{W,R,\text{road}}[i]$ are adjusted for best representation of measurements. As the focus is on vehicle emission, the measurement set-up is chosen according to the standard geometry with a horizontal distance of 7.5 m and a microphone height of 1.2 m [11]. By measuring sound pressure of a vehicle pass-by, only total noise can be observed. A separation in propulsion and rolling noise as needed for direct estimation of the model parameters is not straightforward. In [12] a method has been proposed to sense noise in the near-field of vehicles which simplifies the evaluation of the different contributions. However this method is only applicable to a limited set of vehicles and therefore not used here.

From an external perspective at the border of the road, a vehicle pass-by can be acoustically characterized by the maximal pass-by level or the sound event level. In freely flowing traffic the main challenge is to separate the vehicle of interest from the neighbor vehicles. In this context evaluation strategies have to be applied that do not statistically distort the sample of considered vehicles [13]. For example, a simple *6 dB level down* validity test features a bias towards noisy vehicles and will exclude silent vehicles systematically with higher probability.

To reliably predict energy based descriptors such as an Leq and to minimize uncertainty in the analysis of random signals [14], a sound event level vehicle characterization

is preferred [10] and chosen here. Assuming an omnidirectional radiation characteristic in the horizontal plane, an equivalent sound power of a point source is determined that induces an event level as measured.

The selection of valid vehicle pass-by events for subsequent evaluation was based on the condition that the temporal separation to the neighbor vehicle was larger than 3 seconds. No level criterion was applied to avoid statistical distortion of the set of considered vehicles. To identify a possible correction, the level time history was inspected for all valid events (Figure 1).

The boundaries for the integration of the event energy were selected as points in time for which a level minimum was reached to both sides of the event maximum (t_1 and t_2 in Figure 1). The integral is erroneous in two aspects. On one hand it contains unwanted energy of the neighbor sources, on the other hand it lacks of a portion of the wanted pass-by event. Fortunately the two errors have opposite signs and thus compensate to some extent. In order to derive a relation between the parameter $\mathrm{dB_{down}}$ that corresponds to the minimum of the level difference between maximum and minimum to both sides of the pass-by peak (Figure 1) and the error of the resulting sound event level, a Monte Carlo simulation was performed. The calculation simulated a highway situation with vehicles traveling on all lanes with speeds ranging from 80 to 120 km/h and temporal separations between 3 and 10 seconds. The vehicles were represented by omnidirectional point sources with an arbitrary variation of the emitted sound power of ± 10 dB. The microphone signal was calculated by consideration of geometrical spreading only. The evaluation of the simulation revealed that the corrected sound event level L'_E can be estimated as

$$L'_E = L_E - 3.3 \cdot \exp\left(-0.2 \cdot \mathrm{dB_{down}}\right), \qquad (5)$$

where L_E corresponds to the integration from t_1 to t_2.

During 17 measurement campaigns at sites with different pavement conditions and at speed regimes varying from 30 to 120 km/h, a total of 700'000 valid vehicle pass-by events were evaluated. This figure splits up into 530'000 passenger cars, 65'000 HGV's, 95'000 delivery vans, 5000 buses and 5000 motorcycles.

Table II exemplarily shows equivalent A-weighted sound power levels $L_W[c]$ and single vehicle standard deviations $\sigma[c]$ (see Equation 2) for the SWISS10 vehicle categories at typical highway speeds on a SMA11 pavement.

3.3. Fitting process

The four A, B model parameters for each third-octave band are adjusted all together in a brute force fitting process to minimize differences between measurements and model. To allow the fitting process to separate propulsion and rolling noise contributions it is essential to include data at high and low speeds and preferably on silent and noisy pavements. To identify the pavement correction $\Delta L_{W,R,\mathrm{road}}[i]$, an iterative process is applied. After a preliminary A, B parameter optimization for all categories, $\Delta L_{W,R,\mathrm{road}}[i]$ is adjusted for best fit. Subsequently the A, B parameter optimization is initiated again but now including the obtained information about the pavement correction. It must be emphasized that the assumption of $\Delta L_{W,R,\mathrm{road}}[i]$ being a pavement property is a prerequisite for the functioning of this method.

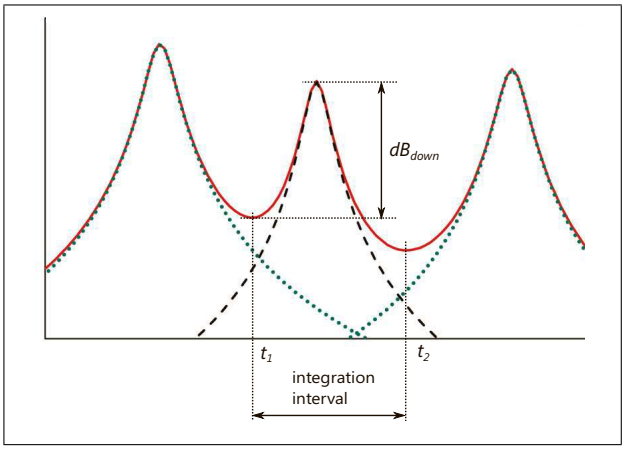

Figure 1. (Colour online) Idealized time history for three point sources passing the microphone. The dashed black curve represents the source of interest, pointed green is the contribution of the unwanted neighbor sources, solid red is the observable total sound pressure.

Table II. Average A-weighted sound power level and single vehicle standard deviation $\sigma[c]$ at typical highway speeds at site Reiden on a SMA11 pavement for the SWISS-10 vehicle categories c.

c	speed [km/h]	$L_W[c]$ [dB(A)]	$\sigma[c]$
1	100	113.1	2.2
2	120	110.7	2.4
3	120	111.9	1.6
4	88	110.9	1.7
5	120	112.6	1.7
6	88	111.8	1.8
7	88	115.0	2.2
8	88	114.7	2.7
9	88	115.9	1.7
10	88	115.6	1.7

4. Model parameter setting

Tables III to VI list the spectral A and B parameter values of propulsion and rolling noise in third octave bands as identified during the fitting process. It turned out that the available data did not allow for a stable estimation of the speed dependency of propulsion noise ($B_P[c, i]$) in categories 1 and 5 to 10. These uncertain values were replaced by the corresponding CNOSSOS values. All parameters are understood for an ACMR8 reference pavement. Figure 2 to 4 show the speed dependent contributions of propulsion and rolling noise to total A-level for motorcycles, passenger cars and trucks. The summation of

Table III. Spectral A_P parameter of the propulsion noise component for the SWISS10 vehicle categories 1 to 10.

freq	cat1	cat2	cat3	cat4	cat5	cat6	cat7	cat8	cat9	cat10
50	99.5	99.1	91.0	91.0	95.5	92.0	92.0	100.6	101.2	99.7
63	98.0	100.6	87.5	87.5	96.5	92.0	92.0	102.2	106.6	106.2
80	96.0	102.2	86.5	86.5	89.5	92.0	92.0	99.7	102.7	101.2
100	94.5	102.2	84.5	84.5	86.0	91.7	91.7	97.6	97.5	96.2
125	99.0	103.8	83.0	83.0	85.0	91.7	91.7	97.0	99.2	98.0
160	90.0	100.6	83.5	83.5	86.0	91.7	91.7	95.9	95.7	95.7
200	86.5	95.9	82.5	82.5	85.0	91.0	91.0	93.9	93.7	91.4
250	95.5	89.7	83.0	83.0	85.0	91.0	91.0	96.0	96.0	93.8
315	95.0	85.0	82.5	82.5	85.0	91.0	91.0	97.6	97.6	96.5
400	96.5	86.6	81.0	81.0	85.0	91.0	91.0	96.0	96.0	97.4
500	92.0	86.6	81.0	81.0	83.5	91.0	91.0	98.0	98.0	99.1
630	91.0	88.1	83.5	83.5	82.5	91.0	91.0	97.4	97.4	96.2
800	92.0	88.1	82.5	82.5	89.0	93.8	93.8	95.6	95.6	95.9
1000	93.5	85.0	79.0	79.0	85.0	93.8	93.8	89.1	89.1	92.0
1250	87.5	85.0	74.0	74.0	80.5	93.8	93.8	86.0	86.0	90.0
1600	85.0	85.0	72.0	72.0	76.0	90.4	90.4	89.5	89.5	88.3
2000	82.0	83.4	73.5	73.5	79.5	90.4	90.4	90.1	90.1	86.3
2500	83.0	83.4	72.5	72.5	80.5	90.4	90.4	88.3	88.3	85.7
3150	81.5	83.4	73.0	73.0	80.0	84.0	84.0	86.0	86.0	85.2
4000	82.0	83.4	70.0	70.0	78.5	84.0	84.0	84.4	84.4	82.6
5000	79.5	83.4	66.5	66.5	77.0	84.0	84.0	83.4	83.4	77.9
6300	77.0	81.9	64.5	64.5	73.5	77.9	77.9	81.5	81.5	67.1
8000	76.5	80.3	60.5	60.5	70.0	77.9	77.9	79.4	79.4	60.0
10k	60.0	80.3	60.0	60.0	68.0	77.9	77.9	77.8	77.8	60.0

Table IV. Spectral B_P parameter of the propulsion noise component for the SWISS10 vehicle categories 1 to 10.

freq	cat1	cat2	cat3	cat4	cat5	cat6	cat7	cat8	cat9	cat10
50	0.0	1.0	0.0	0.0	0.0	0.0	0.0	1.0	1.0	1.0
63	0.0	1.6	0.0	0.0	0.0	0.0	0.0	1.0	1.0	1.0
80	0.0	3.5	0.0	0.0	0.0	0.0	0.0	1.0	1.0	1.0
100	3.0	3.5	7.2	7.2	4.7	4.7	4.7	3.0	3.0	3.0
125	3.0	3.5	7.2	7.2	4.7	4.7	4.7	3.0	3.0	3.0
160	3.0	7.8	7.2	7.2	4.7	4.7	4.7	3.0	3.0	3.0
200	4.6	9.7	7.7	7.7	6.4	6.4	6.4	4.6	4.6	4.6
250	4.6	9.0	7.7	7.7	6.4	6.4	6.4	4.6	4.6	4.6
315	4.6	9.0	7.7	7.7	6.4	6.4	6.4	4.6	4.6	4.6
400	5.0	9.0	8.0	8.0	6.5	6.5	6.5	5.0	5.0	5.0
500	5.0	7.8	8.0	8.0	6.5	6.5	6.5	5.0	5.0	5.0
630	5.0	8.3	8.0	8.0	6.5	6.5	6.5	5.0	5.0	5.0
800	5.0	9.7	8.0	8.0	6.5	6.5	6.5	5.0	5.0	5.0
1000	5.0	9.7	8.0	8.0	6.5	6.5	6.5	5.0	5.0	5.0
1250	5.0	9.4	8.0	8.0	6.5	6.5	6.5	5.0	5.0	5.0
1600	5.0	7.8	8.0	8.0	6.5	6.5	6.5	5.0	5.0	5.0
2000	5.0	8.9	8.0	8.0	6.5	6.5	6.5	5.0	5.0	5.0
2500	5.0	9.7	8.0	8.0	6.5	6.5	6.5	5.0	5.0	5.0
3150	5.0	9.7	8.0	8.0	6.5	6.5	6.5	5.0	5.0	5.0
4000	5.0	9.2	8.0	8.0	6.5	6.5	6.5	5.0	5.0	5.0
5000	5.0	8.3	8.0	8.0	6.5	6.5	6.5	5.0	5.0	5.0
6300	5.0	9.7	8.0	8.0	6.5	6.5	6.5	5.0	5.0	5.0
8000	5.0	9.7	8.0	8.0	6.5	6.5	6.5	5.0	5.0	5.0
10k	5.0	9.7	8.0	8.0	6.5	6.5	6.5	5.0	5.0	5.0

Table V. Spectral A_R parameter of the rolling noise component for the SWISS10 vehicle categories 1 to 10.

freq	cat1	cat2	cat3	cat4	cat5	cat6	cat7	cat8	cat9	cat10
50	83.9	84.0	85.5	90.0	87.0	92.6	93.8	87.8	92.6	92.6
63	97.2	93.4	90.5	95.8	89.0	96.4	101.9	90.0	91.8	91.8
80	96.9	93.4	90.5	93.5	91.5	94.9	99.6	90.0	90.7	90.7
100	94.3	90.2	88.4	91.1	88.4	91.3	93.8	89.9	91.8	91.8
125	82.3	88.7	86.5	90.4	90.0	89.4	94.8	90.4	92.5	92.5
160	93.8	85.5	84.9	88.5	89.4	85.7	93.4	91.6	92.2	92.2
200	98.8	93.2	85.3	88.6	88.8	86.0	93.6	92.9	94.2	94.2
250	91.9	93.4	86.0	89.9	89.0	86.1	95.1	91.8	90.9	90.9
315	86.4	91.8	86.0	89.7	88.0	89.5	101.5	97.6	91.3	91.3
400	90.2	90.4	86.6	90.2	87.6	92.2	100.8	99.1	97.2	97.2
500	96.1	88.9	87.2	90.9	89.7	94.0	101.7	98.3	97.8	97.8
630	97.1	87.3	88.2	94.2	91.7	96.2	104.0	101.9	101.4	101.4
800	98.6	87.6	92.5	98.0	94.5	98.9	104.9	103.3	104.4	104.4
1000	97.1	89.2	95.0	97.9	97.0	97.7	102.3	102.1	102.3	102.3
1250	96.1	90.8	94.0	96.9	95.0	97.0	100.0	100.6	100.3	100.3
1600	94.5	89.0	92.3	96.2	93.3	96.6	98.2	98.4	98.3	98.3
2000	92.6	88.9	90.7	93.9	90.7	93.6	95.4	95.7	95.7	95.7
2500	89.8	87.0	87.4	90.7	87.4	89.3	91.4	92.0	92.9	92.9
3150	86.6	85.2	84.1	87.5	84.1	87.8	89.5	89.4	89.9	89.9
4000	83.6	83.0	81.0	84.3	81.0	84.0	86.3	87.1	87.6	87.6
5000	81.5	80.9	77.5	81.1	77.5	79.7	82.3	82.7	84.9	84.9
6300	80.7	79.1	74.7	79.6	76.7	80.5	82.2	80.9	83.7	83.7
8000	79.7	78.8	72.4	78.6	75.4	79.2	81.1	79.1	82.5	82.5
10k	78.4	75.4	69.6	76.3	73.1	76.7	79.4	77.1	80.6	80.6

Table VI. Spectral B_R parameter of the rolling noise component for the SWISS10 vehicle categories 1 to 10.

freq	cat1	cat2	cat3	cat4	cat5	cat6	cat7	cat8	cat9	cat10
50	25.0	25.0	25.0	25.0	25.0	25.0	25.0	25.0	25.0	25.0
63	38.1	25.0	25.0	25.0	25.0	25.0	25.0	40.0	40.0	40.0
80	40.0	25.0	27.3	27.3	27.0	27.0	27.0	40.0	40.0	40.0
100	40.0	25.0	29.5	29.5	25.0	25.0	25.0	25.0	25.0	25.0
125	25.0	25.5	36.5	36.5	30.0	30.0	30.0	25.0	25.0	25.0
160	32.0	25.0	36.4	36.4	28.0	28.0	28.0	25.0	25.0	25.0
200	25.0	25.0	32.0	32.0	25.0	25.0	25.0	25.0	25.0	25.0
250	25.0	37.2	25.0	25.0	25.0	25.0	25.0	34.0	25.0	25.0
315	40.0	37.7	25.0	25.0	28.9	28.9	28.9	40.0	40.0	40.0
400	40.0	38.1	25.3	25.3	25.1	25.1	25.1	40.0	40.0	40.0
500	40.0	35.3	26.6	26.6	25.0	25.0	25.0	40.0	40.0	40.0
630	40.0	35.3	32.0	32.0	25.0	25.0	25.0	40.0	40.0	40.0
800	40.0	37.7	31.0	31.0	28.9	28.9	28.9	40.0	40.0	40.0
1000	40.0	38.6	33.1	33.1	30.5	30.5	30.5	28.8	40.0	40.0
1250	39.6	35.3	38.7	38.7	34.0	34.0	34.0	27.5	40.0	40.0
1600	40.0	36.7	39.5	39.5	35.8	35.8	35.8	27.7	40.0	40.0
2000	38.9	33.0	39.8	39.8	39.3	39.3	39.3	32.0	40.0	40.0
2500	37.3	30.6	39.8	39.8	39.8	39.8	39.8	40.0	40.0	40.0
3150	39.3	26.9	39.8	39.8	39.8	39.8	39.8	36.0	40.0	40.0
4000	40.0	25.0	38.0	38.0	39.8	39.8	39.8	31.2	40.0	40.0
5000	39.4	25.0	36.8	36.8	39.8	39.8	39.8	40.0	40.0	40.0
6300	40.0	25.5	39.8	39.8	39.8	39.8	39.8	40.0	40.0	40.0
8000	40.0	25.0	39.8	39.8	39.8	39.8	39.8	40.0	40.0	40.0
10k	40.0	29.7	39.8	39.8	39.8	39.8	39.8	40.0	40.0	40.0

the third-octave band powers to an A-level followed the weighting according to IEC 61672-1 (2013). A comparison between CNOSSOS and sonROAD18 is shown in Figure 5 (passenger cars) and Figure 6 (HGVs). The CNOSSOS calculations used reference conditions while the sonROAD18 prediction was obtained for an AC11 pavement and with a correction for 20°C air temperature. The resulting third octave band values of sonROAD18 were combined to corresponding octave bands for direct comparison with CNOSSOS.

5. Vertical directivity

Vertical directivity $\Delta L_{W,\theta}[c, i]$ accounts for the fact that sound radiation reduces with increasing elevation angles θ, [2]. This effect is more pronounced for high frequencies. Consideration of vertical directivity is relevant in cases where elevated receiver points are close to the road or for the accurate prediction of the effect of noise barriers close to the road. Based on measurements with 8 microphone channels at different heights taken at four sites with average speeds of 50 and 80 km/h, an arbitrary directivity function as shown in Equation (6) was derived.

$$\Delta L_{W,\theta}[c, f] = D_1[c] \sin(\theta)^3 \cdot \left(\lg(f) + D_2[c] \right)^3, \qquad (6)$$

where f is frequency and usually chosen as center frequency of the third octave band i of interest. For passenger cars (SWISS10-cat3) the parameters were determined as D_1 = -0.11, D_2 = 0.0 (Figure 7). This setting is also applied to SWISS10 categories 4 to 7. For SWISS10-cat8 vehicles the setting was found as D_1 = -0.04, D_2 = 1.6. This setting is also applied to SWISS10 categories 1, 9 and 10. For motorcycles (SWISS10-cat2) omnidirectional directivity is assumed: $\Delta L_{W,\theta}[2, f] = 0$.

SonROAD18 assumes omnidirectional directivity in the horizontal plane for the prediction of Leq-based indicators. To account for the fact that rolling noise radiation is weaker under 90°, a specific correction is applied in the estimation of maximal pass-by levels (Section 9).

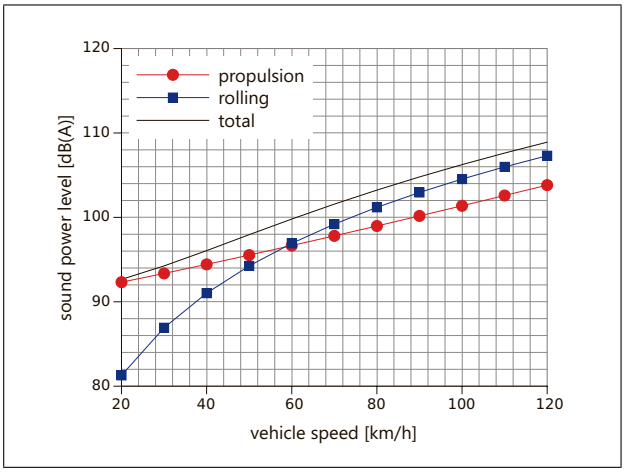

Figure 2. Propulsion, rolling and total noise as a function of vehicle speed for SWISS10-cat2 vehicles (motorcycles) on the reference pavement ACMR8.

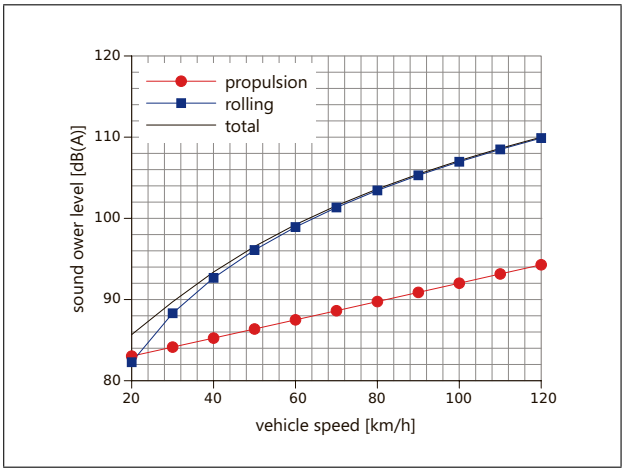

Figure 3. Propulsion, rolling and total noise as a function of vehicle speed for SWISS10-cat3 vehicles (passenger cars) on the reference pavement ACMR8.

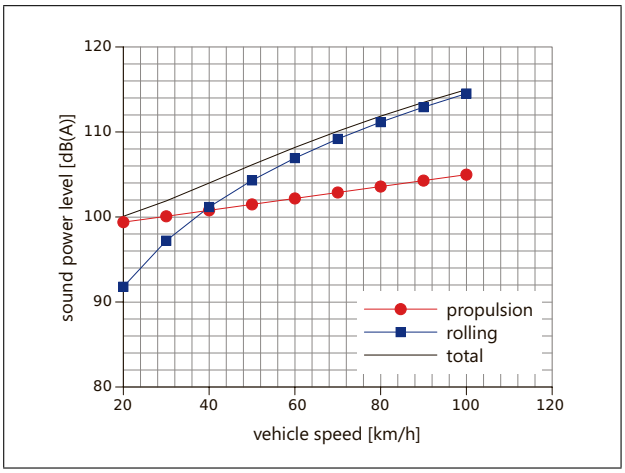

Figure 4. Propulsion, rolling and total noise as a function of vehicle speed for SWISS10-cat8 vehicles (heavy goods vehicle) on the reference pavement ACMR8.

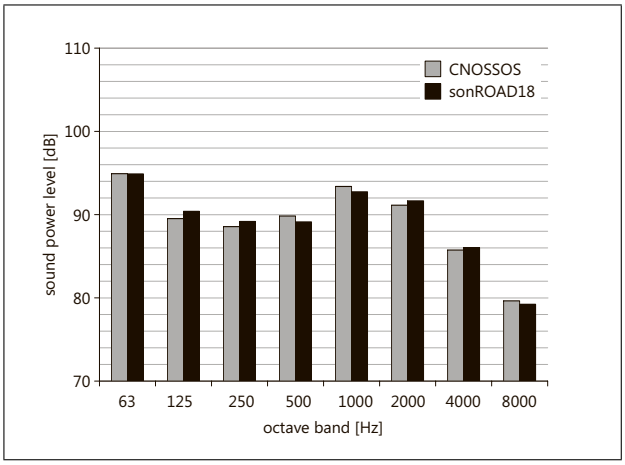

Figure 5. Sound power spectrum of total noise of a passenger car at 50 km/h according to CNOSSOS at reference conditions and according to sonROAD18 on an AC11 pavement at 20°C.

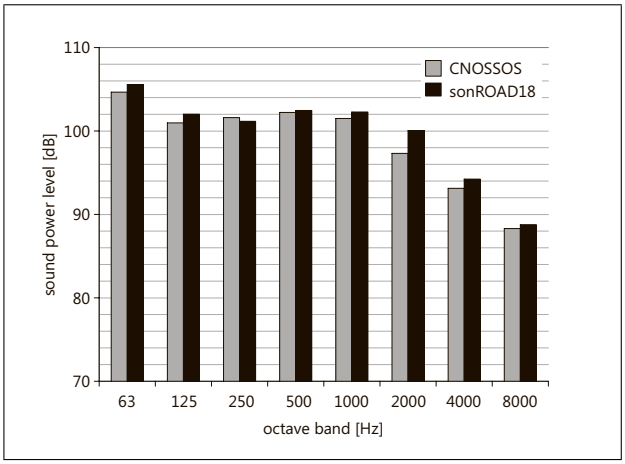

Figure 6. Sound power spectrum of total noise of a HGV at 50 km/h according to CNOSSOS at reference conditions and according to sonROAD18 on an AC11 pavement at 20°C.

6. Electric vehicles

Electric and combustion engine vehicles obviously differ in their propulsion noise. On top of that, emission differences in rolling noise may occur due to particular tyres used with electric vehicles.

A literature review reveals several studies concerning the noise emission of electric vehicles. Within the COMPETT project (Competitive Electric Town Transport) a survey was carried out in 2013 [15] and results of additional measurements are presented in [16]. Results of the recent EU project FOREVER are published in [17, 18, 19, 20]. The studies [17] and [19] propose an adaptation of propulsion noise in CNOSSOS-EU for electric and hybrid vehicles. Correction factors are provided for each octave band (see Table VII). However, as total noise is usually dominated by rolling noise anyhow, it was decided in sonROAD18 to fully ignore propulsion noise in electric vehicles.

From a survey with 19 Swiss agencies of car manufacturers regarding the tyres mounted on electric or hybrid vehicles can be concluded that in general no special tyres are chosen for electric vehicles. There is only a weak trend towards tyres with a low rolling resistance. This corresponds to the findings in the FOREVER study. Furthermore no correlation between rolling resistance and noise emission of the tyres was found [18]. In line with the most recent studies [19, 20] can be concluded that electrical and combustion engine vehicles do not significantly differ in their rolling noise.

No acoustic vehicle alerting system (AVAS) is considered here. With the obligation for new electric vehicles in 2019 the effect on total noise emission has to be reconsidered.

7. Validation of the model

Subsequently to the parameter fitting process, the model was validated with 17 independent measurement campaigns at stationary driving conditions and with microphone locations close to the road. They covered the whole range of vehicle speeds from 30 to 120 km/h, a set of different pavement types and different road gradients. The comparison between measurement and calculation was evaluated with respect to the A-weighted energy equivalent sound pressure level $L_{\mathrm{eq},A}$ of total traffic over a time period of 30 minutes up to 48 hours close to the road. The prediction by the model used information about the geometry, the pavement type, the vehicle speeds and the traffic densities in each vehicle category. As the distances to the microphone were small, a simplified propagation model was used that accounted for geometrical spreading and atmospheric absorption only.

The standard error over the 17 situations was found as 1.5 dB(A). The differences between calculation and measurement range from −1.9 to +1.0 dB(A). Detailed results are presented in Table VIII.

8. Uncertainty of the model

The estimation of the model uncertainty requires a specification of the quantity of interest. From a typical application perspective it seems meaningful to consider the prediction of an average energy equivalent sound pressure level at a specific location and evaluated during a time period that guarantees the incorporation of a sufficiently large sample of the vehicle fleet.

The uncertainty is determined by the following two types of errors:

model errors due to uncertainties of the empirical model description and the fact that some effects and influencing factors are neglected,

input data errors due to missing or inaccurate knowledge of input data.

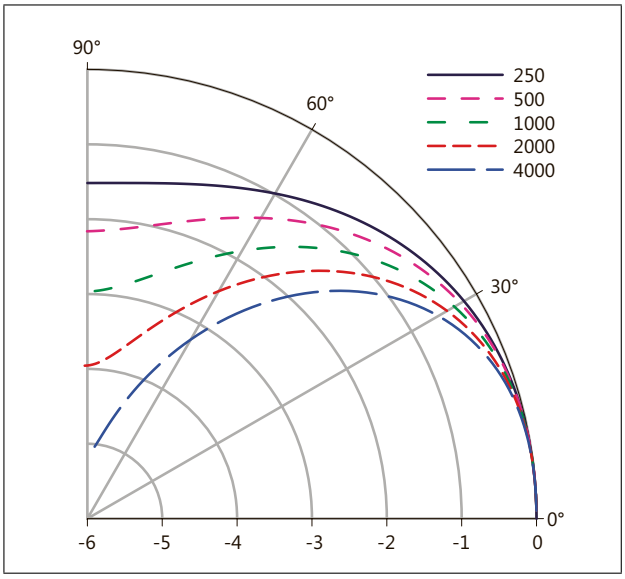

Figure 7. Polar plot of vertical directivity $\Delta L_{W,\theta}$ of SWISS10-cat3 vehicles (passenger cars) for frequencies 250 Hz to 4000 Hz in octave steps.

Table VII. Correction factors *Corr* to be applied to the propulsion noise component of light vehicles in all-electric mode [19].

Octave [Hz]	125	250	500	1000	2000	4000
Corr [dB]	-1.7	-4.2	-15	-15	-15	-13.8

Table VIII. Difference between measured and calculated $L_{\mathrm{eq},A}$ for the different validation situations.

v [km/h]	slope [%]	pavement	$\Delta L_{\mathrm{eq},A(\mathrm{calc-meas})}$
30	3	AC 11	+1.0
30	0	ACMR 8	-0.4
30	5	ACMR 8	+1.0
50	7	AC 11S	-0.9
50	5	AC 8S	-1.5
50	3	AC 11	-1.0
50	6	SMA 11	-0.9
50	0	AB 11	-0.6
50	7	AC 11	-1.9
50	13	SMA 11	-1.3
50	8	AB 11	-1.7
80	0	AC 11	-0.6
80	0	PMA	-1.2
80	2	ACMR 8	-1.7
100	0	SDA 8	-1.6
120	0	SDA 8	-0.1
120	0	SMA 11	+0.5

8.1. Model errors

Model errors describe the uncertainty of the emission level prediction assuming all the necessary input data is available. Here we focus on stationary vehicle operating conditions and exclude scenarios with accelerating vehicles that show increased variability. Thus a full description of a situation provides information about

- average speed of the vehicles in each category,
- traffic density in each category,
- pavement type,
- slope of the road,
- air temperature.

As described above, the evaluation of the available set of validation measurements with full knowledge of the input data and comparison with the model prediction yielded a standard error of 1.5 dB(A).

This figure can be considered as the inherent model error. As rolling noise is very relevant in most situations, an important source of uncertainty is insufficient knowledge about the pavement properties. Indeed, measurements show substantial scatter of rolling noise emission within one pavement type. The gold standard in pavement description is information derived from passing vehicles at the road side. Methods in use are CB (coast-by, EU Directive 2001/43/EC), SPB (statistical pass-by, ISO 11819-1) or CPB (controlled pass-by, NF S31-119-2). Useful information to improve accuracy of the pavement correction can also be derived from CPX measurements (Close ProXimity, ISO 11819-2), however the conversion of CPX data into road side emission values involves again a substantial uncertainty [21].

8.2. Input data errors

The application of an emission model for noise mapping purposes usually lacks of complete knowledge of the necessary input data. A sensitivity analysis is therefore instructive to demonstrate the relevance of each input parameter with respect to the accuracy of the emission value.

As a prediction task we understand here the calculation of the A-weighted, energy equivalent sound pressure level $L_{\mathrm{eq},A}$ at a receiver in the reference distance of 7.5 m according to

$$L_{\mathrm{eq},A} = 10\lg\left(\sum_{c=1}^{10}\frac{N[c]}{v[c]}\cdot\sum_{i=1}^{n}10^{0.1(L_W[c,i]+A'[i])}\right)+K, \quad (7)$$

where $L_W[c,i]$ is the sound power level of a vehicle of category c at speed $v[c]$ in the third octave band i, $N[c]$ is the number of vehicles per hour and $A'[i]$ is the A-weighting including air absorption, K is a constant.

The evaluation of the sensitivities requires the specification of an operating point. Here three test cases are considered as reference situations from which the model parameters are varied:

quarter, 30 km/h one lane of a quarter road with a speed limit of 30 km/h on a AC8 pavement with typical split into different vehicle classes,

urban, 50 km/h one lane of an urban road on a AC8 pavement with a speed limit of 50 km/h and typical split into different vehicle classes,

highway, 120 km/h one normal lane of a four lane highway on a AC8 pavement with a speed limit of 120 km/h and typical split into different vehicle classes.

Table IX. Sensitivity analysis of an $L_{\mathrm{eq},A}$ calculation with respect to different input parameters for three scenarios: quarter, urban and highway.

parameter	quarter	urban	highway	
speed v_m	0.5	0.9	1.2	dB/10%
slope s	0.2	0.1	0.05	dB/1%
$\Delta L_{W,R,\mathrm{road}}$	0.5	0.8	1.0	dB/1dB
temp. T	-0.3	-0.6	-0.7	dB/10°
traffic N	0.4	0.4	0.4	dB/10%

Table IX lists the numerically evaluated sensitivities for a calculation according to Equations (1), (3), (4) and (7). The values are obtained by comparison of two runs, one with the original input parameter setting and one with a modification as indicated in Table IX.

9. Estimation of maximal pass-by levels

sonROAD18 characterizes the emission of a vehicle by the radiated sound power level L_W of a representative, in the horizontal plane omnidirectional point source. This approach yields correct prediction of energy based quantities such as L_{eq} or L_{den} but may fail in estimating maximal pass-by levels L_{max}. Jonasson [2] proposed a non-uniform directivity for the rolling noise component. Own measurements suggest an adjustment that has to be applied to total noise. Based on 15 campaigns that covered different speed regimes and different pavement types, a correction factor $\Delta K_{\mathrm{max,A}}$ was determined to relate A-weighted sound power level $L_{W,A}$ and A-weighted maximal pass-by level $L_{\mathrm{max,7.5m,A}}$ in a distance d of 7.5 m (the term "-8" represents the conversion of sound power level into sound pressure level on a hemisphere of radius 1 m),

$$\begin{aligned} L_{\mathrm{max,7.5m,A}} &= L_{W,A} - 20\log(d) - 8 + \Delta K_{\mathrm{max,A}} \\ &= L_{W,A} - 25.5 + \Delta K_{\mathrm{max,A}}. \end{aligned} \quad (8)$$

Figure 8 shows the correction factors derived for each measurement for passenger cars and delivery vans.

For vehicle categories $c = 3...6$ the speed dependency of $\Delta K_{\mathrm{max,A}}$ can be estimated according to Equation (9). For c = 1,2,7...10, $\Delta K_{\mathrm{max,A}} = 0$ can be concluded from the observations.

$$\Delta K_{\mathrm{max,A}} = 0.9 - 0.0227\cdot v \quad , \quad v \geq 20\ \mathrm{km/h}. \quad (9)$$

10. Temporal spacing

Although of no relevance for energy considerations, the temporal spacing between two neighbor vehicles is of importance when it comes to auralisations [22],[23], [24],[25] the investigation of annoyance or sleep disturbance [26], [27] or the evaluation of indicators that consider temporal aspects of sound pressure [28], [29], [30]. Based on evaluations of traffic counter data, a statistical model for the temporal spacing between neighbor vehicles

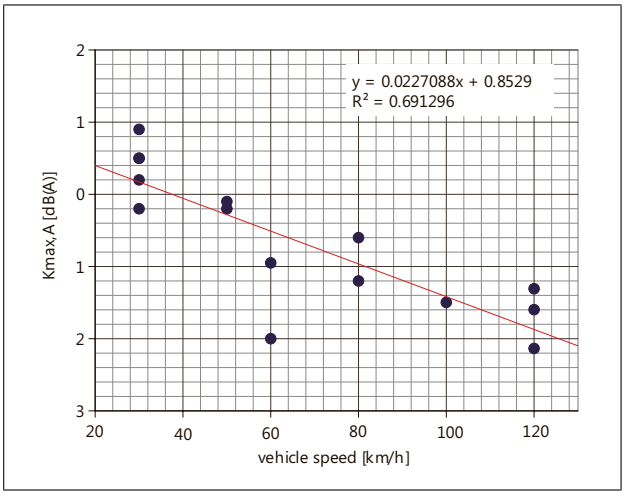

Figure 8. Maximal level correction factors $\Delta K_{\mathrm{max,A}}$ and linear regression line for passenger cars and delivery vans as a function of vehicle speed.

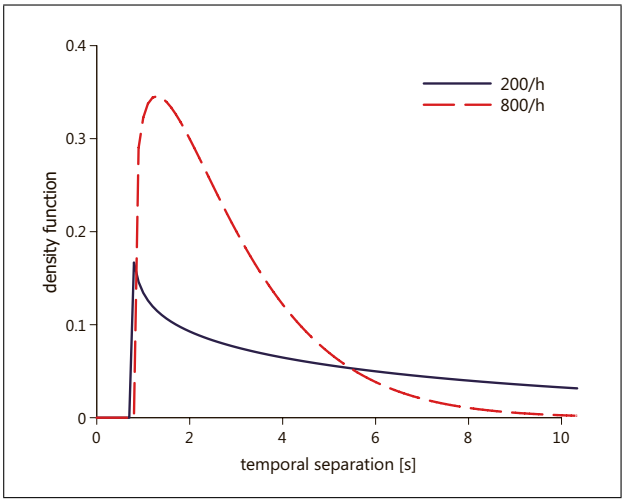

Figure 9. Exemplary Weibull density function for a main road with allowable speed 80 km/h for two traffic densities 200 and 800 vehicles/hour per lane.

was deduced. It was found that the density functions can be satisfactorily approximated by a three parameter (α, β and μ) Weibull distribution. For $x \geq \mu$ the density function $f(x)$ is given by Equation (10), for $x < \mu$ $f(x) = 0$.

$$f(x) = \frac{\alpha}{\beta}\left(\frac{x-\mu}{\beta}\right)^{\alpha-1} \cdot \mathrm{e}^{-\left(\frac{x-\mu}{\beta}\right)^{\alpha}}. \qquad (10)$$

Figure 9 shows an exemplary Weibull density function, Table X to XII list the parameters for different road types.

11. Interface to propagation models

The chosen specification of emitted sound power already includes the reflection at the ground in the vicinity of the source. Consequently in the propagation calculation no additional ground effect has to be considered for receiver distances up to 7.5 m.

Table X. Weibull parameter α, β and μ in dependency of the traffic density N in vehicles per hour per lane for freely flowing traffic at 50 km/h on a main road.

N_{lane}	α	β	μ
100	0.85	20.00	0.7
200	0.85	9.59	0.7
400	1.01	4.29	0.9
800	1.04	1.97	0.8

Table XI. Weibull parameter for freely flowing traffic at 80 km/h on a main road.

N_{lane}	α	β	μ
100	0.81	20.00	0.7
200	0.83	10.80	0.7
400	1.02	3.96	0.8
800	1.20	2.18	0.8

Table XII. Weibull parameter for freely flowing traffic at 120 km/h on the normal lane of a four-lane highway.

N_{lane}	α	β	μ
100	1.24	20.00	0.5
200	1.02	15.13	0.8
400	1.12	7.52	0.6
800	1.28	3.77	0.5
1600	1.41	1.80	0.4

The analysis of the spectral ground effect according to ISO 9613-2 for an incoherent line source at 0.05 m above hard ground reveals for receiver distances of 7.5 m and receiver heights ranging from 1.2 to 4 m values between +3.0 and +3.2 dB. The link to the ISO 9613-2 propagation model can thus be established with sufficient accuracy by subtracting 3 dB from the emission levels and subsequent regular application of the propagation model.

The link to more general ground effect calculation schemes that explicitly evaluate the interference pattern between direct and ground reflected sound [31] is established in sonROAD18 by the introduction of a fully absorbing ground zone that stretches 7.5 m to both sides of the line source. Figure 10 shows the exemplary ground effect for grass land adjacent to the road.

12. Conclusions

Based on a large data set of single vehicle pass-by measurements, the CNOSSOS road traffic noise emission model was adapted to the Swiss vehicle fleet and the classification scheme SWISS10. In order to account for horizontal directivity that shows up at high vehicle speeds, the sound event level of vehicle passings was used as acoustical indicator. It was found that in general the observed total noise could be successfully split up into a propulsion and a rolling noise component by a brute force parameter optimization to minimize differences between model and

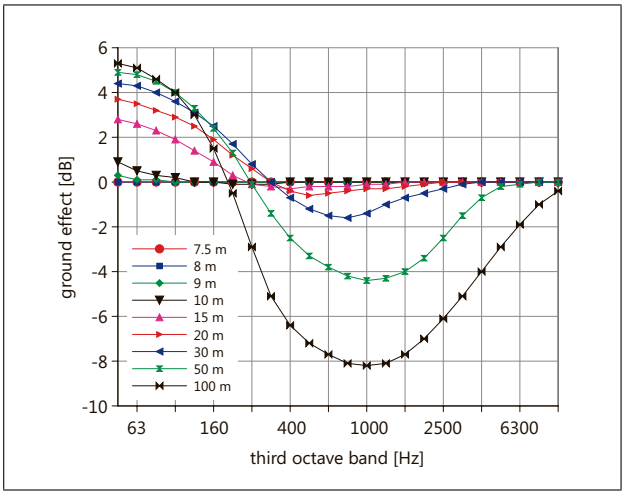

Figure 10. Spectral ground effect for an absorbing source zone of 7.5 m width and adjacent grassland for a receiver at 4 m height in different distances.

measurement. In some vehicle categories the speed dependency of the propulsion noise component B_P was difficult to estimate and thus set according to CNOSSOS. A prerequisite for the separation of propulsion and rolling noise is the inclusion of measurements that differ with respect to vehicle speeds, road gradients and pavement types. In contrast to CNOSSOS, sonROAD18 takes vertical directivity into account. Although the sensitivity of the emission with respect to the elevation angle is not very large, the effect is systematic and may become relevant in the calculation of barrier attenuation or receiver level calculations for positions high up and close to the road.

In situations with full knowledge of the model input parameters and a pavement specification by its type, a prediction uncertainty of 1.5 dB in the sense of a standard deviation was found. The major contribution to this uncertainty is the variation of performance of the pavement within a pavement class. A reduction of the prediction uncertainty can be achieved by inclusion of specific pavement corrections based on measurements. To this end, a conversion model is under development that allows to translate spectral CPX measurements into pavement corrections.

Acknowledgement

This work was initiated and financed by FOEN, the Swiss Agency for the Environment.

References

[1] S. Kephalopoulos, M. Paviotti, F. Anfosso-Ledee: Common Noise Assessment Methods in Europe (CNOSSOS-EU). 2012.

[2] H. G. Jonasson: Acoustical Source Modelling of Road Vehicles. Acta Acust united Ac **93** (2007) 173–184.

[3] Computermodell zur Berechnung von Strassenlaerm, Bedienungsanleitung StL-86, Schriftenreihe Umweltschutz Nr. 60, Bundesamt fuer Umweltschutz, Schweiz, 1987.

[4] K. Heutschi: SonRoad: New Swiss road traffic noise model. Acta Acust united Ac **90** (2004) 548–554.

[5] K. Heutschi, B. Locher: sonROAD18 - Berechnungsmodell für Strassenlärm, im Auftrag des Bundesamtes für Umwelt (BAFU), Schweiz, 2018.

[6] A. L. Brown, D. Tomerini: Distribution of the noise level maxima from the pass-by of vehicles in urban road traffic streams. ROAD & Transport Research **20** (2011) 41–54.

[7] L. Estévez-Mauriz, J. Forssén: Dynamic traffic noise assessment tool: A comparative study between a roundabout and a signalised intersection. Applied Acoustics **130** (2018) 71–86.

[8] A. Can, P. Aumond: Estimation of road traffic noise emissions: The influence of speed and acceleration. Transportation Research Part D: Transport and Environment **58** (2018) 155–171.

[9] ASTRA Richtlinie 13012, Verkehrszähler, Bundesamt für Strassen, ASTRA, 2009.

[10] S. J. Shilton, F. Anfosso Ledee, H. van Leeuwen: Conversion of existing road source data to use CNOSSOS-EU, 469-474, EuroNoise 2015.

[11] ISO 11819-1 Acoustics - Measurement of the influence of road surfaces on traffic noise - Part 1: Statistical Pass-By method, 1997.

[12] D. Ibarra, R. Ramirez-Mendoza, E. Lopez: A New Approach for Estimating Noise Emission of Automotive Vehicles. Acta Acust united Ac **102** (2016) 930–937.

[13] K. Heutschi: On Single Event Measurements of Heavy Road Vehicles in Freely Flowing Traffic. Acta Acust united Ac **94** (2008) 709–714.

[14] J. T. Broch: Principles of experimental frequency analysis, Elsevier Science Publishers, 1990.

[15] L. M. Iversen, G. Marbjerg, H. Bendtsen: Noise from electric vehicles - 'state-of-the-art' literature survey, Internoise, 2013.

[16] R. S. H. Skov, L. M. Iversen: Noise from electric vehicles - measurements, COMPETT WP3, 2015.

[17] M. A. Pallas, M. Bérengier, M. Muirhead, P. Morgan: How to consider Electric and Hybrid Electric vehicles in CNOSSOS-EU predicting method?, Proceedings of Forum Acusticum, 2014.

[18] S. Gasparoni, M. Czuka, R. Wehr, M. Conter, M. A. Pallas, M. Bérengier: FOREVER Impact of low-noise tyres on electric vehicle noise emission, WP3 Final Report, 2015.

[19] M. A. Pallas, M. Bérengier, R. Chatagnon, M. Czuka, M. Conter, M. Muirhead: Towards a model for electric vehicle noise emission in the European prediction method CNOSSOS-EU, Applied Acoustics **113** (2016) 89–101.

[20] M. Czuka, M. A. Pallas, P. Morgan, M. Conter: Impact of potential and dedicated tyres of electric vehicles on the tyre-road noise and connection to the EU noise label, Proceedings of 6th Transport Research Arena, 2016.

[21] J. Cesbron, P. Klein: Correlation between tyre/road noise levels measured by the Coast-By and the Close-ProXimity methods. Applied Acoustics **126** (2017) 36–46.

[22] R. Pieren, T. Bütler, K. Heutschi: Auralization of accelerating passenger cars using additive synthesis. Applied Sciences **6** (2016).

[23] J. Forssén, T. Kaczmarek, J. Alvarsson, P. Lundén, M.E. Nilsson: Auralization of traffic noise within the LISTEN project - Preliminary results for passenger car pass-by. Pro-

ceedings of the Eighth European Conference on Noise Control, Edinburgh, UK, 26–28 October 2009.

[24] J. Maillard, J. Jagla: Real Time Auralization of Non-Stationary Traffic Noise - Quantitative and Perceptual Validation in an Urban Street. Proceedings of the AIA-DAGA Conference on Acoustics, Merano, Italy, 18–21 March 2013.

[25] J. Forssén, A. Hoffmann, W. Kropp: Auralization model for the perceptual evaluation of tyre-road noise. Applied Acoustics **132** (2018) 232–240.

[26] L. Gille, C. Marquis-Favre, A. Klein: Noise Annoyance Due To Urban Road Traffic with Powered-Two-Wheelers: Quiet Periods, Order and Number of Vehicles. Acta Acust united Ac **102** (2016) 474–487.

[27] B. Schaffer *et al.*: Short-term annoyance reactions to stationary and time-varying wind turbine and road traffic noise: A laboratory study. J. Acoustical Society of America **139** (2016) 2949–2963.

[28] B. De Coensel *et al.*: A model for the perception of environmental sound based on notice-events. J. Acoustical Society of America **126** (2009) 656–665.

[29] J. M. Wunderli *et al.*: Intermittency ratio: A metric reflecting short-term temporal variations of transportation noise exposure. J. Exposure Science and Environmental Epidemiology **26** (2016) 575–585.

[30] A. L. Brown, B. De Coensel: A study of the performance of a generalized exceedance algorithm for detecting noise events caused by road traffic. Applied Acoustics **138** (2018) 101–114.

[31] D. C. Hothersall, J. B. N. Harriott: Approximate models for sound propagation above multi-impedance plane boundaries. J. Acoustical Society of America **97** (1995) 918–926.

[32] ISO 9613-2 Acoustics - Attenuation of sound during propagation outdoors, Part 2: General method of calculation, 1996.